The Journal of Experimental Biology 204, 543–557 (2001)
Printed in Great Britain © The Company of Biologists Limited 2001
JEB3077

PREY-CAPTURE BEHAVIOR IN GYMNOTID ELECTRIC FISH: MOTION ANALYSIS AND EFFECTS OF WATER CONDUCTIVITY

MALCOLM A. MACIVER[1,2], NOURA M. SHARABASH[2] AND MARK E. NELSON[1,2,3,*]

[1]*The Neuroscience Program,* [2]*Beckman Institute for Advanced Science and Technology,* and [3]*Department of Molecular and Integrative Physiology, University of Illinois at Urbana-Champaign, Urbana, IL 61801, USA*

*Author for correspondence (e-mail: m-nelson@uiuc.edu)

Accepted 3 November 2000; published on WWW 15 January 2001

Summary

Animals can actively influence the content and quality of sensory information they acquire from the environment through the positioning of peripheral sensory surfaces. This study investigated receptor surface positioning during prey-capture behavior in weakly electric gymnotiform fish of the genus *Apteronotus*. Infrared video techniques and three-dimensional model-based tracking methods were used to provide quantitative information on body position and conformation as black ghost (*A. albifrons*) and brown ghost (*A. leptorhynchus*) knifefish hunted for prey (*Daphnia magna*) in the dark. We found that detection distance depends on the electrical conductivity of the surrounding water. Best performance was observed at low water conductivity (2.8 cm mean detection distance and 2 % miss rate at 35 μS cm^{-1}, *A. albifrons*) and poorest performance at high conductivity (1.5 cm mean detection distance and 11 % miss rate at 600 μS cm^{-1}, *A. albifrons*). The observed conductivity-dependence implies that nonvisual prey detection in *Apteronotus* is likely to be dominated by the electrosense over the range of water conductivities experienced by the animal in its natural environment. This result provides the first evidence for the involvement of electrosensory cues in the prey-capture behavior of gymnotids, but it leaves open the possibility that both the high-frequency (tuberous) and low-frequency (ampullary) electroreceptors may contribute. We describe an electrosensory orienting response to prey, whereby the fish rolls its body following detection to bring the prey above the dorsum. This orienting response and the spatial distribution of prey at the time of detection highlight the importance of the dorsal surface of the trunk for electrosensory signal acquisition. Finally, quantitative analysis of fish motion demonstrates that *Apteronotus* can adapt its trajectory to account for post-detection motion of the prey, suggesting that it uses a closed-loop adaptive tracking strategy, rather than an open-loop ballistic strike strategy, to intercept the prey.

Key words: computational neuroethology, electrolocation, electroreception, active sensing, conductivity, sensory ecology, nonvisual orienting behaviour, mechanosensory lateral line, backwards locomotion, reverse swimming, motion capture.

Introduction

One universal task carried out by the nervous system is the extraction and enhancement of sensory signals that are relevant to behavior. This sensory acquisition process has both motor and sensory aspects. The motor aspect is related to the positioning of peripheral receptor surfaces, providing the animal with some degree of control over the content and quality of incoming sensory data. The sensory aspect is related to the adaptive filtering of incoming data for further enhancement of relevant signal components and suppression of extraneous signals. For the electrosensory system, prey detection and localization provide a neuroethological context for studying both sensory and motor aspects of sensory acquisition (MacIver et al., 1997; Nelson and MacIver, 1999).

This study presents a quantitative analysis of the positioning of peripheral receptor surfaces during the detection and capture of small aquatic prey in two species of South American gymnotid weakly electric knifefish, *Apteronotus albifrons* (black ghost) and *A. leptorhynchus* (brown ghost). Weakly electric fish possess an organ that produces an electric discharge (electric organ discharge; EOD). In *Apteronotus*, the EOD creates a quasi-sinusoidal electric field with a fundamental frequency of approximately 1 kHz and a field strength of approximately 1 mV cm^{-1} near the fish.

These fish have the ability to sense both the self-generated electric field and extrinsic electric fields using two submodalities of electrosense, each with a distinct receptor population. The high-frequency electrosense, sensitive to fields similar to the fish's own EOD, is mediated by tuberous receptors, whereas the low-frequency electrosense, sensitive to fields of approximately 0–40 Hz, is mediated by ampullary receptors (for a review, see Zakon, 1986). In active electrolocation behavior, the fish uses its high-frequency electrosense to detect perturbations in the self-generated field (for reviews, see Bastian, 1986; von der Emde, 1999). In

passive electrolocation behavior, the fish uses its low- and high-frequency electrosense to detect extrinsic electric fields such as the weak bioelectric field of aquatic prey or the EODs of other electric fish (Naruse and Kawasaki, 1998; Wilkens et al., 1997; Kalmijn, 1974; Hopkins et al., 1997).

Black and brown ghost knifefish are primarily nocturnal hunters that feed on insect larvae and small crustaceans (Marrero, 1987; Winemiller and Adite, 1997; Mérigoux and Ponton, 1998). Such prey may stimulate the high-frequency electrosense because of the difference in impedance between their bodies and the surrounding water and the low-frequency electrosense because of their bioelectric fields. The prey may also stimulate other nonvisual modalities, such as the mechanosensory lateral line system and the olfactory system.

In weakly electric fish, active electrolocation is often assumed to play a key role in the detection and capture of prey. This assumption is based on the observation that these animals are able to capture prey in the absence of visual cues, as well as the predominance of peripheral receptors and volume of brain tissue devoted to the high-frequency electrosense. In an adult *A. albifrons*, for example, there are approximately 15 000 tuberous receptor organs distributed over the body surface compared with approximately 700 ampullary receptor organs and approximately 300 neuromasts for the mechanosensory lateral line (Carr et al., 1982). Although such indirect arguments for active electrolocation may be compelling, there is currently no direct supporting evidence for electrosensory involvement in prey detection in South American gymnotids, and few studies address this question in African mormyrids (von der Emde, 1994; von der Emde and Bleckmann, 1998).

In this study, we used infrared video recording and a model-based animal tracking system (MacIver and Nelson, 2000) to provide quantitative information on the position and conformation of the fish body and, hence, of the peripheral sensor array during prey-capture behavior. We manipulated the electrosensory contributions to prey-capture behavior by varying water conductivity. Our results provide the first direct evidence for the involvement of electrosensory signals in the prey-capture behavior of gymnotids. We also obtain quantitative data addressing how weakly electric fish orient their sensory surfaces during prey-capture behavior and show that they are able to adapt their strike trajectory to compensate for prey movement. The quantitative behavioral data obtained in these studies provide a link between the motor aspects of sensory acquisition, the adaptive neural processing of electrosensory signals and the sensory ecology of the animal (Nelson and MacIver, 1999; Ratnam and Nelson, 2000).

Materials and methods

Behavioral apparatus

Two adult *Apteronotus albifrons* and two *Apteronotus leptorhynchus*, 12–15 cm in length, were housed in a rectangular Plexiglas aquarium with a central area partitioned from the rest of the tank to form a 40 cm×30 cm×20 cm behavioral observation arena. The arena was imaged by two video cameras that provided top and side views, allowing three-dimensional reconstruction of behavioral trajectories. Video signals from the two cameras were electronically merged and recorded onto video tape for subsequent analysis. To eliminate visual cues, prey-capture behavior was observed using infrared (880 nm) illumination provided by high-intensity infrared diodes. The illuminators, cameras and aquarium were housed within a light-tight enclosure that was maintained on a 12 h:12 h light:dark photoperiod. Water temperature was maintained at 28±1.0 °C and pH 7.0±0.1. Animal care procedures were reviewed and approved by the Laboratory Animal Care and Advisory Committee of the University of Illinois at Urbana-Champaign. For details of the behavioral apparatus, see MacIver and Nelson (MacIver and Nelson, 2000).

Experimental protocol

The prey used in these studies were mature *Daphnia magna* (water fleas), 2–3 mm in length, cultured in our laboratory. *Daphnia magna* are aquatic crustaceans that are similar to the prey typically found in stomach content analyses of *Apteronotus* spp. (Marrero, 1987; Winemiller and Adite, 1997; Mérigoux and Ponton, 1998). Each day, shortly after the beginning of the dark cycle, one fish at a time was allowed into the central observation arena for 15–20 min. Prey were introduced one at a time at random locations near the surface of the tank using a thin flexible tube from outside the light-tight enclosure. This method avoided entry of visible light and generated minimal mechanical disturbance. After introduction of the *Daphnia magna*, its position was observed on the video monitor. If the prey was eaten by the fish or drifted to a corner or bottom of the tank, another prey item was introduced.

We maintained constant water conductivity during each of four sets of recording sessions, each lasting 10–21 days. Behavior was recorded at four different water conductivities: 35±5, 100±5, 300±40 and 600±40 $\mu S\,cm^{-1}$ (sequence 300, 100, 300, 600 and 35 $\mu S\,cm^{-1}$). For each conductivity tested, the behavioral tank water conductivity was established by mixing deionized water with a stock salt solution consisting of $CaSO_4{\cdot}2H_2O$, $MgSO_4{\cdot}7H_2O$, KCl, $NaH_2PO_4{\cdot}H_2O$ and NaCl in a mass ratio of 60:4.7:3.0:1.0:0.8 (L. Maler, personal communication; similar to Knudsen, 1975). Changes between different conductivity values were made gradually, over several days, followed by several days at the new conductivity to acclimate the fish before behavioral data were recorded. Conductivity measurements were made using a calibrated conductivity meter (TDSTestr 40, Cole Parmer Instrument Company, Vernon Hills, IL, USA), and water conductivity was corrected on a daily basis.

Behavioral sequence selection

Videotaped recordings of prey-capture behavior were visually scanned to identify sequences to be digitized for further processing. The criteria for selection of a prey-capture event were as follows: (i) a successful capture, or a failed

capture attempt where there was an abrupt and directed movement towards the prey; (ii) fish and prey visible in both camera views, except for brief occlusions; and (iii) prey at least 2 cm from the bottom and sides of the tank.

The start of a video sequence was typically chosen to begin approximately 0.5 s prior to the onset of the prey strike. The sequence ended with prey capture or, in the rare cases where the fish did not catch the prey, near the time when the mouth of the fish came closest to the prey.

Behavioral data acquisition, visualization and analysis

Selected video sequences were digitized and stored as eight-bit grayscale image files for analysis. The video sampling rate was 60 images s^{-1}, with each video image consisting of one video field with alternate scan lines interpolated. A model-based animal tracking system was developed to determine accurately the trajectory and conformation of the fish's body and the prey position for each image of selected sequences (MacIver and Nelson, 2000). In this system, an accurate three-dimensional 'wireframe' model of the observed fish and prey was overlaid onto digitized images. The fish and prey models were then manipulated by the user to achieve congruence with the side- and top-view images of the actual fish and prey. Calibrated image transformations ensured that model-to-image matching resulted in accurate (±1 mm) recovery of the positions of the animals in the behavioral arena. The fish models were provided with eight degrees of freedom (Fig. 1). The six rigid-body degrees of freedom were the position of the (*x*, *y* and *z*) snout, yaw, pitch and roll (θ, ϕ and Ω). The two nonrigid degrees of freedom were lateral tail bend and dorsoventral bend. The prey was modeled with three degrees of freedom, corresponding to the coordinates of its center. The wireframe fish models were scaled to each individual fish. The output of the model-based tracking system was the value of each model parameter for the fish and prey at each image of the sequence (for further details, see MacIver and Nelson, 2000).

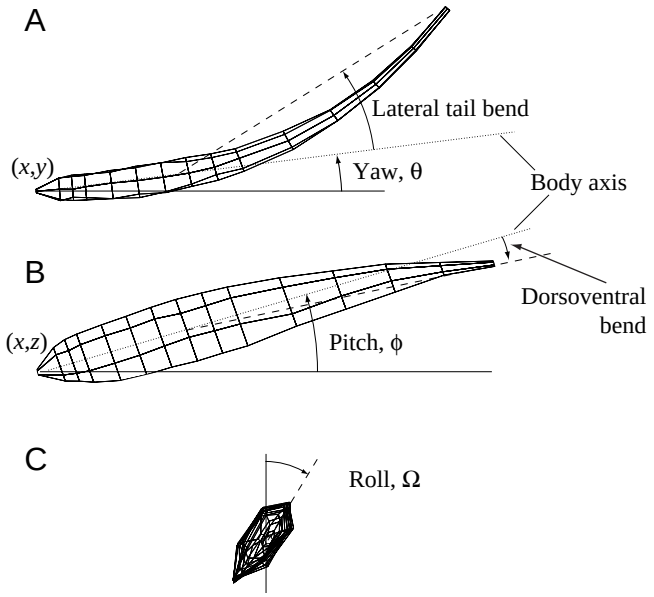

Fig. 1. The fish body model with eight degrees of freedom. (A) Top view showing four degrees of freedom: in-plane position of the snout (*x*,*y*); yaw angle (θ) and lateral tail bend. (B) Side view showing three additional degrees of freedom: vertical position of the snout (*z*), pitch angle (ϕ) and dorsoventral bend. (C) Front view showing roll angle (Ω). The dotted line indicates the central body axis of the unbent fish; yaw (θ) and pitch (ϕ) measure the angle of the body axis relative to the tank coordinate system. Lateral bend angle is defined as the angle in the dorsal plane between the unbent body axis and a line extending from one-third of the body length from the head to the tail; dorsoventral bend is defined as the angle in the median sagittal plane between the unbent body axis and a line extending from one-third of the body length from the head to the tail.

Some analyses presented below required fitting the fish and prey model to images over the entire behavioral sequence (full motion analysis), whereas other analyses required only the less time-intensive process of fitting the single frame in which the fish changed from forward to reverse swimming (single-frame analysis).

Full three-dimensional reconstructions of selected sequences were displayed on computer monitors using a custom-designed prey-strike browser that simultaneously displayed graphs of movement parameters. However, the limited depth cues provided by monitor projections made interpretation of the movements difficult. In collaboration with Stuart Levy of the National Center for Super Computing Applications (NCSA, Beckman Institute, University of Illinois at Urbana-Champaign, http://virdir.ncsa.uiuc.edu/virdir/), we brought the model-based tracking data into an immersive multi-person virtual reality system (CAVE, Fakespace Systems Inc., Kitchener, ON, Canada) (Leigh et al., 1995; Cruz-Neira et al., 1992; Cruz-Neira et al., 1993). The prey-strike browser and CAVE were used to identify patterns of movement that were largely inaccessible in the original video recordings.

Velocities and accelerations were computed using the difference in fitted model positions between successive images. The longitudinal velocity (*u*) of the fish was computed by taking the vector dot product of the snout velocity vector with a heading vector **u**, taken from the yaw (θ) and pitch (ϕ) angles:

$$u_x = -\cos\theta\cos\phi\,, \tag{1a}$$

$$u_y = -\sin\theta\cos\phi\,, \tag{1b}$$

$$u_z = -\sin\phi\,. \tag{1c}$$

The minimum distance between the surface of the fish and the prey was determined by finding the shortest distance between the prey and each of the 84 quadrilateral faces of the fitted wireframe fish model using a parametric optimization procedure.

The time of detection of the prey was taken as the zero-crossing of the longitudinal acceleration profile prior to a rapid reversal in swimming direction (see below). For depictions of prey position at the time of detection (see Figs 5, 6), the coordinates of the fish and prey were transformed into a coordinate frame in which the fish body was straightened and scaled to unit length. Population peri-detection statistics were computed by aligning trials at the time of detection (see Results)

and averaging across trials from 500 ms before the time of detection to 1000 ms after the time of detection. The tails of these peri-detection distributions have reduced values of *N* because of differences in start and end times between trials. All post-detection averages were computed by first aligning trials at the specified post-detection time. All computations were carried out using MATLAB and the image processing, optimization and signal processing tool boxes (The Mathworks Inc., Natick, MA, USA), running on a Unix workstation.

All statistical values are reported as mean ± S.D. unless indicated otherwise. For comparison of receptor surface area and size between *A. albifrons* and *A. leptorhynchus*, the scaled polygonal fish models used for model-based tracking were measured using three-dimensional modeling software (Rhinoceros, Robert McNeel and Associates, Seattle, WA, USA).

Results

In total, 130 *A. albifrons* prey-capture sequences were processed for full motion analysis, with a mean duration of 1.2±0.3 s. In a typical sequence, the fish initially swam forwards and then made a rapid reversal in swimming direction to capture the prey. Such rapid reversals were associated with prey-capture behavior and were rarely observed during normal swimming when no prey were present in the tank.

Fig. 2A shows the longitudinal velocity profile for a representative prey-capture sequence, illustrating a rapid reversal. The time at which the longitudinal velocity changes sign from positive to negative (Fig. 2A, dotted vertical line) is referred to as the 'time of reversal'. The mean duration of a rapid reversal (from time of reversal to time of next forward movement) for all trials was just under half a second (418±141 ms). To obtain a better estimate of the time of prey detection, we used the longitudinal acceleration profile (Fig. 2B) to determine when the fish began to slow down. The zero-crossing of the longitudinal acceleration profile prior to the rapid reversal (Fig. 2B, solid vertical line) was taken as the 'time of detection'. The actual time of detection, however, would be prior to this behavioral response because of neuromotor output delays. In subsequent analyses, these two time points ('time of reversal' and 'time of detection') are used as reference points for comparing distances to prey. Typically, the prey were captured in just over half a second following the time of detection (665±165 ms). Fig. 2C shows the minimum distance between the prey and the surface of the fish, computed from the model-based tracking data. At the time of detection, the *Daphnia* was 3.5 cm away from the sensory surface, and at the time of reversal it was 3.1 cm away.

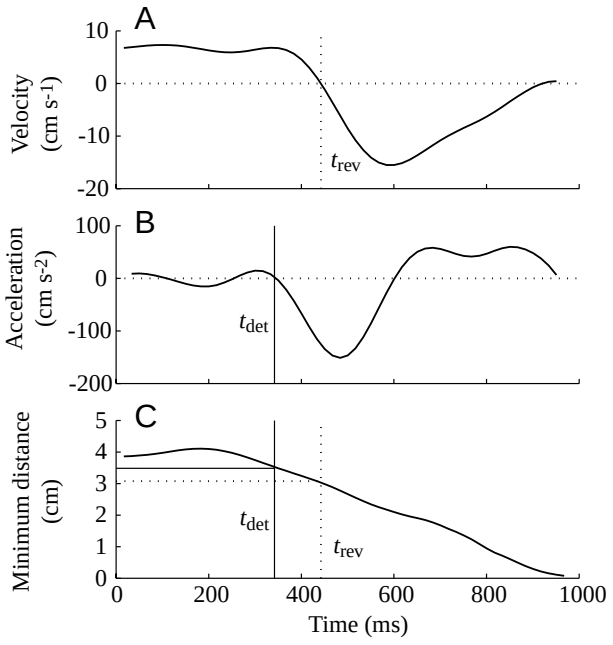

Fig. 2. Longitudinal velocity, longitudinal acceleration and the shortest distance between the prey and the fish body surface for a representative trial that ends with a successful capture. (A) Longitudinal velocity, showing the time of reversal of swimming direction (t_{rev}). (B) Longitudinal acceleration, showing the time of detection of the prey (t_{det}). (C) The shortest distance from the fish body to the prey, with time of reversal (t_{rev}; dotted vertical line), time of detection (t_{det}; solid vertical line), reversal distance (dotted horizontal line) and detection distance (solid horizontal line) indicated.

Longitudinal velocity and acceleration

In 14 of the 130 behavioral sequences, we could not

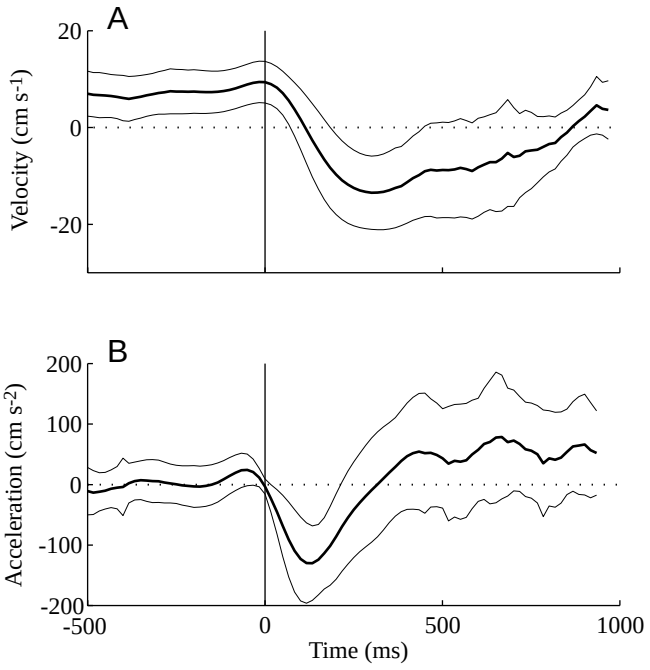

Fig. 3. Population distribution of peri-detection velocity and acceleration for all trials. Values are means (thick solid lines) and standard deviation (thin solid lines) (*N*=116). Trials are aligned at the time of detection (*t*=0 ms), indicated by a vertical line. (A) Longitudinal velocity. (B) Longitudinal acceleration.

determine the time of detection, either because there was no rapid reversal or because the deceleration profile was ambiguous. The other 116 behavioral sequences had velocity and acceleration profiles similar to those shown in Fig. 2.

Fig. 3 shows a peri-detection plot of the average longitudinal velocity and acceleration for all 116 trials, aligned at the time of detection. At the time of detection, the average forward longitudinal velocity of the fish was 9.6±4.3 cm s^{-1}. The peak negative velocity of the rapid reversal occurred on average 307±135 ms following detection and had a magnitude of −19.1±5.2 cm s^{-1}. The average peak reverse acceleration during the rapid reversal was −172±75 cm s^{-2}.

We found that the mean longitudinal velocity from the start of the behavioral segment to the time of detection (pre-detection or search velocity) was 8.1±3.7 cm s^{-1} (N=116). At 35 μS cm s^{-1}, the mean search velocity was significantly higher (10.4±3.3 cm s^{-1}, N=38) than at all other conductivities, with no significant difference between velocities at 100 μS cm s^{-1} and above ($P \leqslant 0.01$, t-test).

Detection distance

In this section, we present results for data collected at 35 μS cm^{-1}, which was associated with the largest mean detection distance. Fig. 4A shows the peri-detection time course of the distance between the fish and prey, averaged over all 35 μS cm^{-1} trials (N=38). The mean distance to the prey at the time of detection was 2.8±0.8 cm. Fig. 4B shows the distribution of distances at the time of detection (range 1.2–5.2 cm). Note that the distribution is well separated from

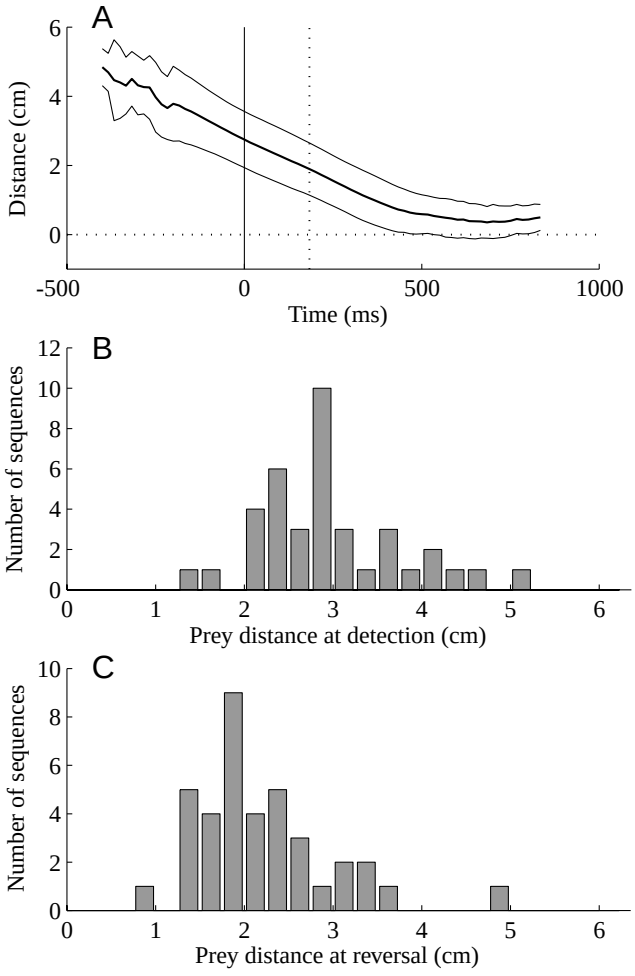

Fig. 4. Detection distance profile and distributions for 35 μS cm^{-1} water conductivity trials (N=38). (A) Mean distance to prey for all trials, aligned at the time of detection (t=0 ms). The vertical solid line indicates the time of detection; the vertical dotted line indicates the average time of fish reversal. Values are means (thick solid lines) and standard deviation (thin solid lines). (B) Histogram showing the detection distance distribution. The mean distance to the prey at the time of detection was 2.8±0.8 cm (mean ± S.D., N=38). (C) Histogram showing the reversal distance distribution. The mean distance to the prey at the time of reversal of swimming direction was 1.9±0.6 cm (mean ± S.D., N=38).

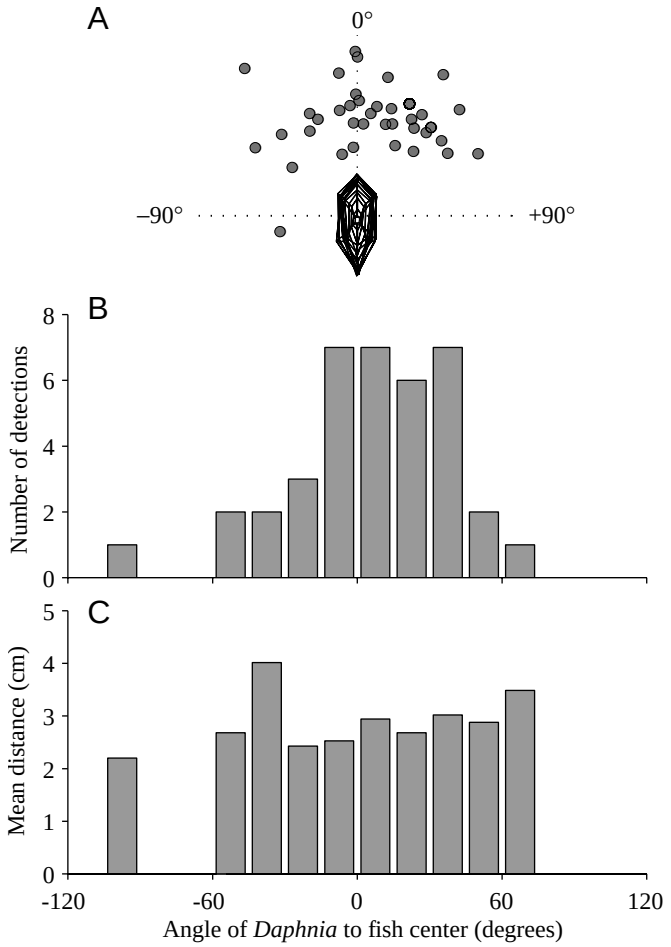

Fig. 5. Angular distribution of the prey around the central axis for 35 μS cm^{-1} water conductivity trials (N=38). Circles indicate the position of the *Daphnia magna* at the time of detection; positive angles are to the animal's right, negative angles are to the animal's left, and 0 ° is the midline above the fish. (A) Tail-on view showing the distribution of the prey at the time of detection. (B) Histogram showing the number of detections at different body angles. (C) Histogram showing the detection distance at different body angles.

the origin, indicating that all detections were non-contact in nature. Fig. 4C shows the distribution of distances at the time of reversal. The distribution is similar to that shown in Fig. 4B, except that the mean is shifted to lower values (1.9±0.6 cm) because the time of reversal occurs approximately 200 ms after the time of detection (see Fig. 2C).

Prey position at time of detection

Most detection events occurred when the prey was close to the dorsal surface of the fish. Figs 5 and 6 illustrate the angular and rostrocaudal distributions of prey at the time of detection for 35 μS cm^{-1} water conductivity. As shown in Fig. 5A, the prey tended to be detected above the dorsal surface of the fish. All prey but two were within ±60 ° of the vertical midline of the fish at the time of detection (Fig. 5B). Mean detection distance did not vary significantly with azimuthal position (Fig. 5C). As shown in Fig. 6A, prey positions were distributed along the entire rostrocaudal extent of the fish. There was a slight bias in the number of detections favoring the anterior trunk region of the fish (Fig. 6B). The mean detection distance did not vary significantly with rostrocaudal position (Fig. 6C).

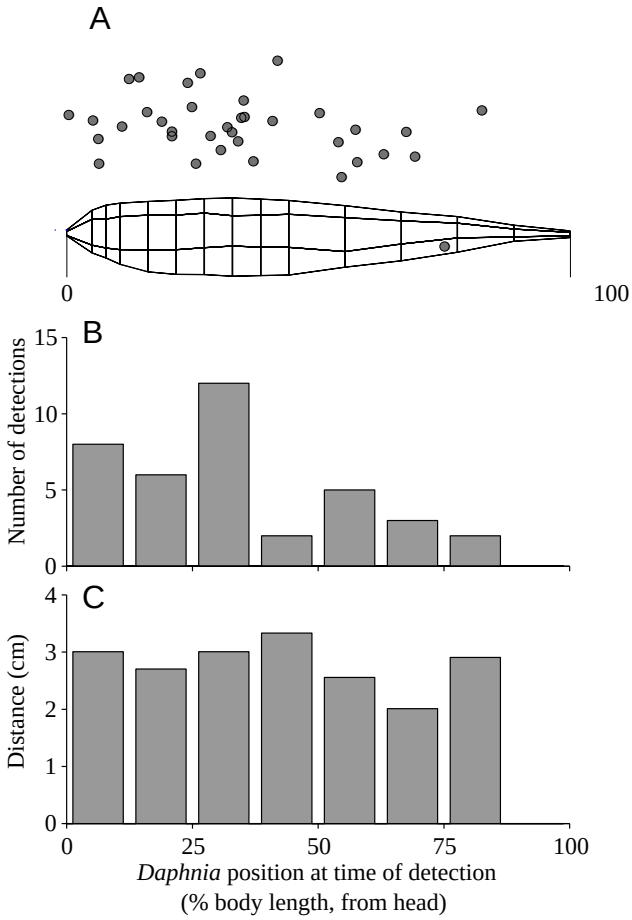

Fig. 6. Rostrocaudal distribution of prey for 35 μS cm^{-1} water conductivity trials (N=38). Body lengths are normalized from 0 (head) to 100 (tail). Circles indicate the position of the *Daphnia magna* at the time of detection. (A) Side view showing the position of the prey at the time of detection projected onto a straightened fish. (B) Histogram showing the number of detections at different body positions. (C) Histogram showing the detection distance at different body positions.

Detection distance and water conductivity

The mean detection distance increased with decreasing water conductivity. At a conductivity of 35 μS cm^{-1}, the mean detection distance was approximately twice that at 600 μS cm^{-1}. Fig. 7A shows the mean and standard deviation of the detection distance distribution for each of the four conductivities tested. The mean detection distances were not significantly different between 300 and 600 μS cm^{-1}, but were significantly different between 300 and 100 and between 100 and 35 μS cm^{-1} (P≤0.01, t-test). Two sets of 300 μS cm^{-1} trials, collected approximately 10 weeks apart, showed no statistically significant difference in mean detection distance and were pooled for this analysis. The results are summarized in Table 1.

The miss rate (misses as a percentage of all capture attempts) decreased monotonically with decreasing water conductivity, from a maximum of 11±3 % at 600 μS cm^{-1} to a minimum of 2±1 % at 35 μS cm^{-1} (mean ± S.E.M.) (Fig. 8). The miss rate at 35 μS cm^{-1} was significantly lower than that at 300 or 600 μS cm^{-1} (P≤0.001, binomial significance test).

Roll and pitch

Prior to detecting prey, fish were typically oriented with a

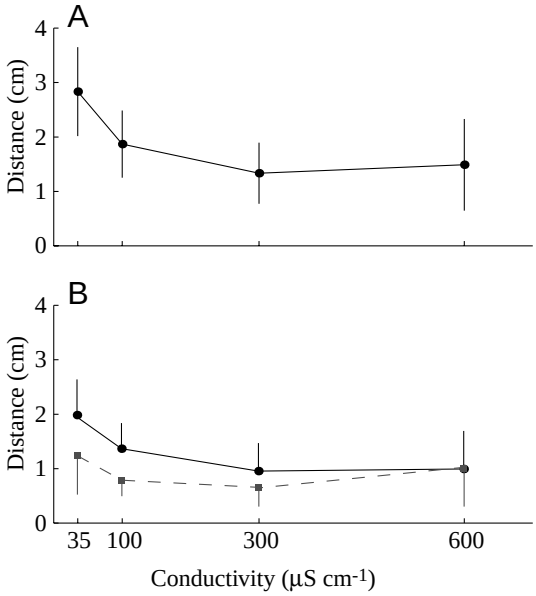

Fig. 7. Detection distance *versus* water conductivity. (A) Distance to prey at the time of detection for *Apteronotus albifrons* from full motion reconstructions. (B) Distance to the prey at the time of reversal of swimming direction from single-frame reconstructions; the solid line is for *A. albifrons*; the dashed line is for *A. leptorhynchus*. Values are means ± S.D.; N values are given in Table 1.

Table 1. *Distance to prey at time of detection and time of reversal for* Apteronotus albifrons *and* A. leptorhynchus

Water conductivity (μS)	Distance to prey (cm)			
	A. albifrons		*A. leptorhynchus*	
	Detection	Reversal	Detection	Reversal
35	2.8±0.8 (38)	1.9±0.6 (54)	1.6±0.8 (12)	1.2±0.7 (34)
100	1.9±0.6 (18)	1.4±0.5 (18)	NA	0.8±0.3 (9)
300	1.3±0.6 (37)	1.0±0.5 (51)	NA	0.6±0.3 (17)
600	1.5±0.8 (23)	1.0±0.7 (23)	NA	1.0±0.7 (20)

Values are means ± S.D. (*N*).
NA, not applicable.

body roll angle close to zero (–3±16°, *N*=116, Fig. 9A). At the end of the rapid reversal (onset of the final forward lunge to engulf the prey), approximately 0.6 s later, the mean roll angle was still close to zero, but the root mean square (RMS) value had increased significantly, from 17 to 33° (Fig. 9A). This post-detection increase in the RMS value is due to rolling movements following detection. A typical rolling movement is illustrated in Fig. 10A.

Fig. 9B compares the change in roll angle (from the time of detection to the time of maximum reverse velocity) with the angle of the prey at the time of detection. The angle to the prey is defined as shown in the inset of Fig. 9B. The slope of the regression line is close to unity, indicating that, between the time of detection and the time of maximum reverse velocity, the fish rolled through approximately the same angle as it initially made to the prey (slope 0.93, $P \leqslant 0.001$). This resulted in the prey being located above the dorsum following the roll movement.

When the fish were searching for prey, they typically swam forward with their bodies pitched slightly downwards. At the time of detection, the average pitch angle was 29±9.8° (Fig. 11). In this posture, the dorsal surface of the trunk forms the leading edge as the fish moves through the water. During the rapid reversal, the pitch angle tended to decrease. At the end of the rapid reversal, approximately 0.6 s after detection, the mean pitch angle had decreased to 15±13°.

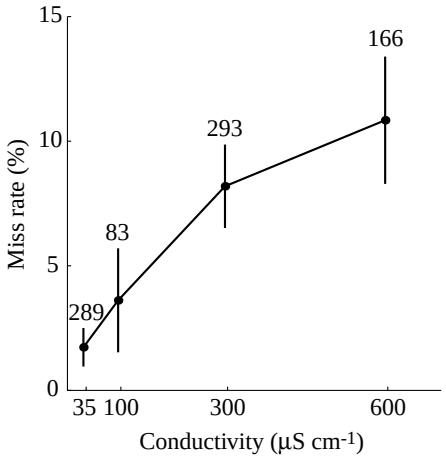

Fig. 8. Comparison of miss rate, defined as failed prey-capture attempts, as a percentage of all prey-capture attempts, at four water conductivities for *Apteronotus albifrons*. Values are means ± S.D., Sample numbers for each data point are indicated on the graph.

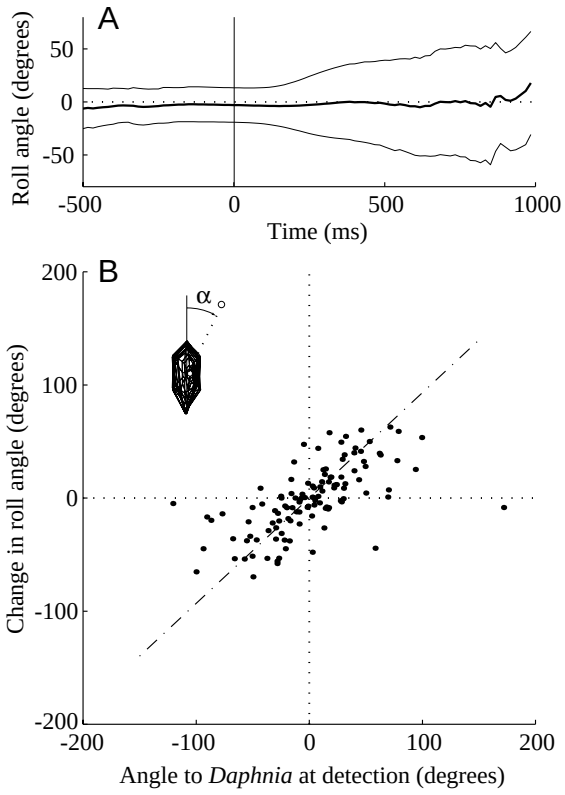

Fig. 9. Peri-detection population distribution of roll angle and evidence for an electrosensory orienting response to prey. (A) Mean (thick solid line) and root mean square (RMS; thin solid lines) values of the roll angle; trials are aligned at the time of prey detection (t=0 ms) indicated by a vertical line. (B) The change in roll angle from the time of detection to the time of maximum reverse longitudinal velocity *versus* the initial angle to the prey at the time of detection (α). The angle to the prey is defined as shown in the inset. The dashed line shows the relationship when the roll angle change is equal to the initial prey angle and corresponds to a linear regression of the data (r^2=0.41, P<0.0001). N=116 capture attempts.

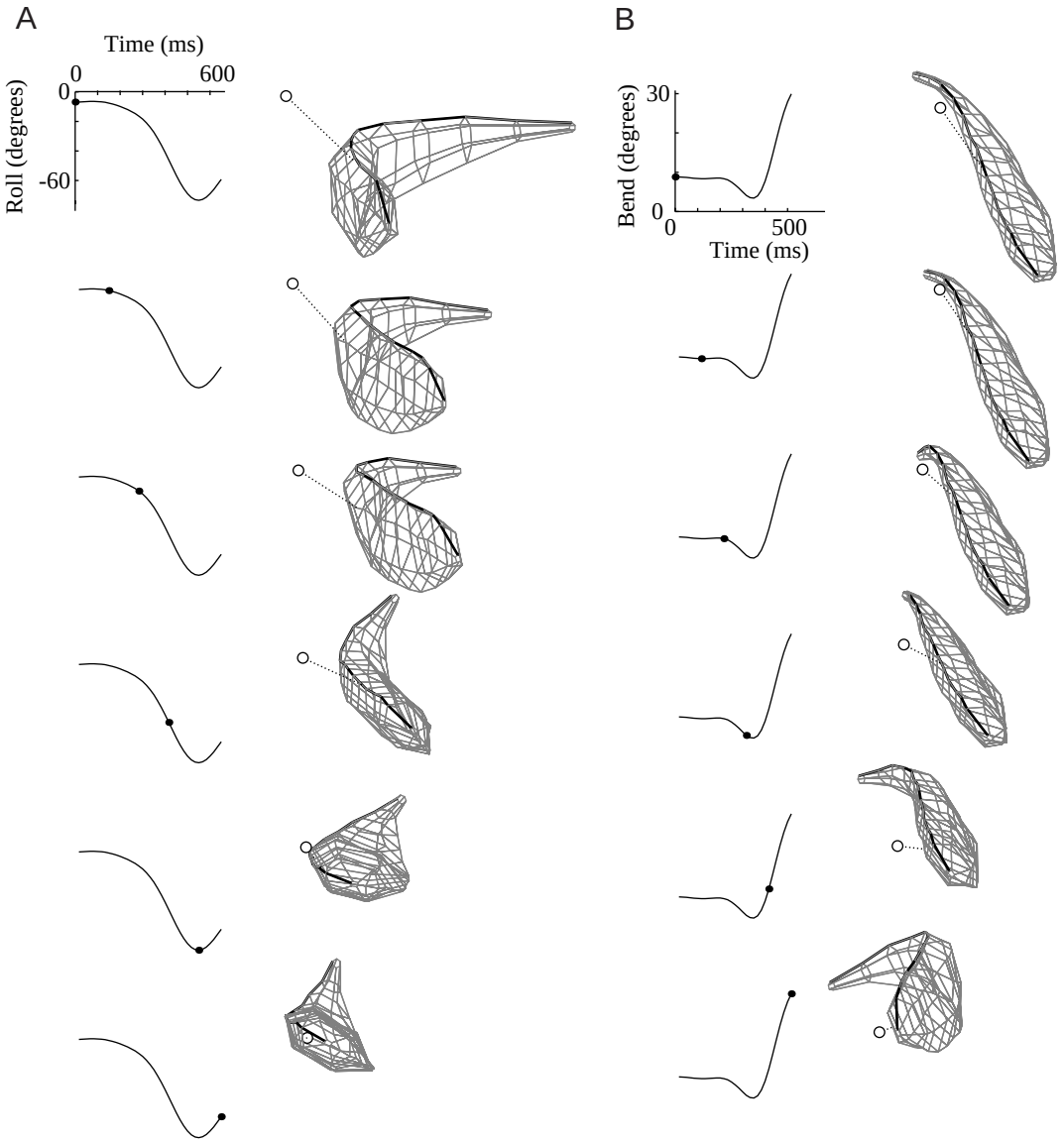

Fig. 10. Two characteristic movement strategies used by the fish during prey-capture behavior are shown in two different prey-capture sequences. In both panels, the top snapshot (t=0 ms) is at the time of detection, and time increases up to the last snapshot at the end of the sequence. The heavy line on the fish indicates the dorsum, the open circle marks the position of the *Daphnia magna*, and the dotted line indicates the shortest distance from the *Daphnia* to the body surface. (A) Roll, a possible electrosensory orienting behavior. The inset plot on the left shows the roll angle history and current value (filled circle). (B) Lateral body bending to swing the mouth rapidly to a laterally positioned *Daphnia*. The inset plot on the left shows the lateral bend angle history and current value (filled circle). Other details as in A.

Lateral tail bend and bending velocity

Following detection, as the fish executed the rapid reversal, the degree of lateral tail bend tended to decrease. The lateral tail bend angle is defined as shown in Fig. 1A. The mean of the lateral bend angle is always near zero (Fig. 12), indicating that the fish showed no preference for left- *versus* right-side body bends. The RMS bend angle, however, dropped significantly following detection. At the time of detection, the RMS value was 31 °, whereas at the end of the rapid reversal approximately 0.6 s later, it had declined to 16 °.

The bend angle analysis provides information about the degree to which the body is bent, but not about how rapidly the bend angle is changing. We examined the lateral bend velocity across all 116 trials and found a mean RMS lateral bend velocity of 107 ° s^{-1} around the time of detection. There was no significant difference between pre- and post-detection values. For a 14 cm *A. albifrons*, this bend velocity corresponds to a tail tip velocity of approximately 19 cm s^{-1}. At the end of a rapid reversal, there was often a rapid dorsoventral or lateral body bend just prior to capture to close the final gap to the prey (Fig. 10B).

Effects of prey displacement on prey-capture behavior

To assess whether fish tended to perform ballistic strikes at

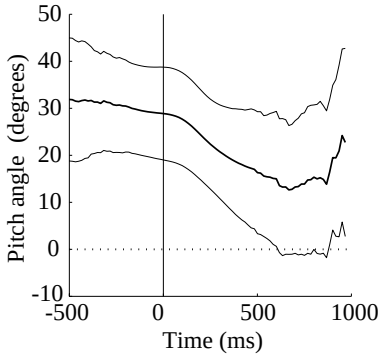

Fig. 11. Mean (thick solid line) and standard deviation (thin solid lines) of the pitch angle for 116 capture attempts; trials are aligned at the time of prey detection (t=0 ms) indicated by a vertical line.

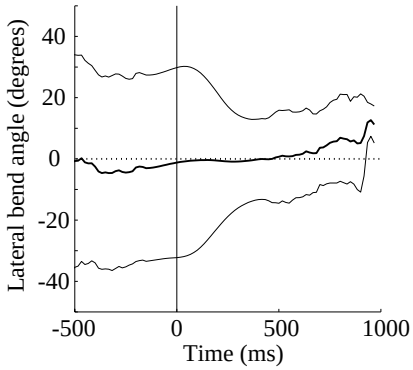

Fig. 12. Mean (thick solid line) and root mean square (RMS; thin solid lines) value of the lateral bend angle for 116 capture attempts; trials are aligned at the time of prey detection (t=0 ms) indicated by a vertical line.

the place where the *Daphnia* was originally detected or whether they were able to modify their strike trajectory to compensate for prey displacement, we examined trials in which the *Daphnia* moved 2.0 cm or more between the time of detection and capture. The mean *Daphnia* displacement from the time of detection to capture was 1.5±1.0 cm, and the prey was displaced 2.0 cm or more in 25 of the 116 trials. For these trials, we compared two distances at each time step following detection: the distance from the mouth of the fish to the (changing) position of the prey, and the distance from the mouth of the fish to the (unchanging) position of the prey at the time of detection. A representative graph of these two quantities and of the corresponding capture sequence is shown in Fig. 13. Fig. 13A shows that the distance from the mouth of the fish to the prey decreased more rapidly than the distance from the mouth of the fish to the original position of the prey at the time of detection. If, as shown in Fig. 13, the distance between the mouth and the actual prey position dropped below 1.0 cm before the distance between the mouth and the original prey position dropped below 1.0 cm, we categorized the trial as an adaptive strike. The converse condition was counted as a ballistic strike. If neither condition was met (e.g. the prey never came closer than 1.0 cm to the mouth because of a failed

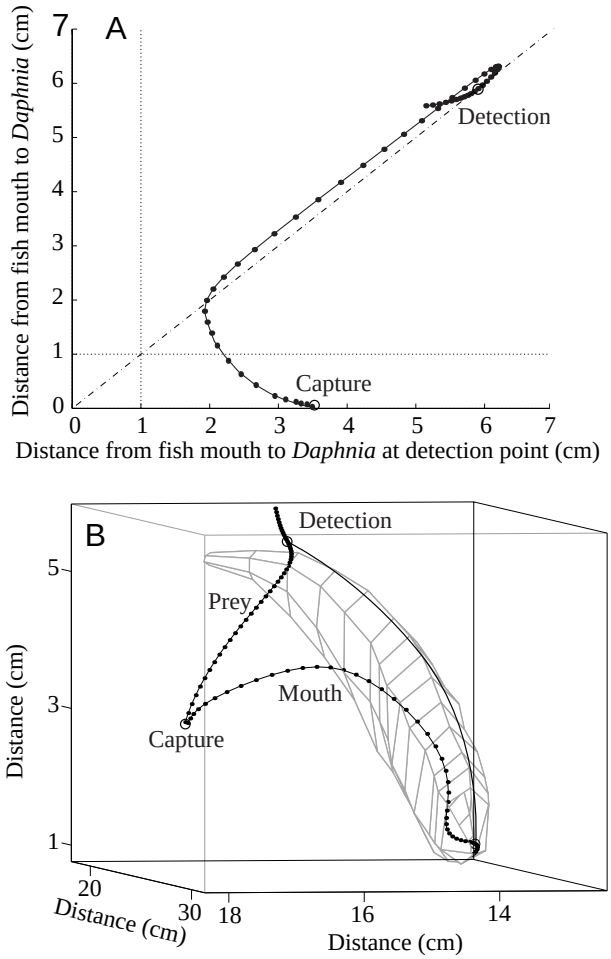

Fig. 13. A sample analysis of one capture in which the *Daphnia magna* was displaced by approximately 4 cm between the time of detection and the time of capture. (A) A parametric plot of the distance from the mouth of the fish to the (changing) prey position *versus* the distance from the mouth of the fish to the (unchanging) original position of the prey at the time of detection. Each point on the curve represents the value for the corresponding video image (60 images s^{-1}; inter-image interval 16.67 ms). The dotted lines at 1.0 cm indicate our threshold for categorizing the sequence as adaptive or ballistic. (B) Illustration of the original positions of the fish and prey and subsequent trajectories for A. If the fish had made a ballistic strike, the head might be expected to have followed a trajectory to the location of the prey at the time of detection, similar to the hypothetical trajectory shown by the solid line. The actual fish trajectory (lower dotted solid line) follows the drift of the prey, intercepting the prey trajectory (upper dotted solid line) at the time of capture.

strike), the trial was scored as inconclusive. By these criteria, 18 of the 25 attempts were categorized as adaptive strikes, two attempts were categorized as ballistic strikes and five attempts were categorized as inconclusive.

Comparison between species

In general, *A. leptorhynchus* exhibited reduced detection performance (shorter detection distances, higher miss rates) than *A. albifrons*. However, the key features of their behavior,

including forward swimming velocity, reversal velocity and acceleration, pitch, tail bend, tail bend velocity and post-detection increase in RMS roll angle were similar to those reported above for *A. albifrons* (N=12, 35 μS cm^{-1}).

To make comparisons between the distance at which prey are sensed in *A. albifrons* and *A. leptorhynchus*, we performed single-frame analyses of the video recordings using the time of velocity reversal as a reference point (see Fig. 2A). Fig. 7B compares the prey distance at the time of reversal for *A. albifrons* (solid lines) and *A. leptorhynchus* (dashed lines). The results are summarized in Table 1. The distance to the prey at the time of reversal was generally larger for *A. albifrons* than for *A. leptorhynchus*. These differences were significant at 35, 100 and 300 μS cm^{-1}, but not at 600 μS cm^{-1} ($P \leqslant 0.05$, t-test). The dependence of detection distance on water conductivity was similar for both species. The mean miss rate for *A. leptorhynchus* was more than twice as high as for *A. albifrons*. *A. leptorhynchus* captured approximately half as many *Daphnia* per session as *A. albifrons* (mean values, four per session for *A. leptorhynchus* and seven per session for *A. albifrons*).

There were several qualitative differences that are not reflected in these data. First, *A. leptorhynchus* appeared less motivated to feed on *Daphnia*. Approximately 800 prey captures were recorded for *A. albifrons*, but only half as many prey captures were recorded for *A. leptorhynchus*. We often observed *A. leptorhynchus* capturing a *Daphnia* and then ejecting it from its mouth; this was never observed with *A. albifrons*. Although we observed that *A. albifrons* increased their general search activity after prey had been detected, this was less apparent with *A. leptorhynchus*. In addition, *A. leptorhynchus* swam backwards more often than *A. albifrons* while searching for prey. Only 4 % of the *A. albifrons* trials were excluded because the animal was moving backwards at the time of detection (preventing identification of the time of detection), whereas 15 % of the *A. leptorhynchus* trials were excluded for this reason.

The surface area and volume of length-matched *A. albifrons* were larger than for *A. leptorhynchus*. A 16 cm *A. leptorhynchus* had a surface area of 34 cm^2 and a volume of 6 cm^3, whereas a 15 cm *A. albifrons* had a surface area of 49 cm^2 and a volume of 10 cm^3. The percentage differences were similar for a 12 cm *A. albifrons* compared with a 12 cm *A. leptorhynchus*.

Discussion

The body of the weakly electric fish serves as a dynamic sensory antenna that can be repositioned to improve the reception of signals of interest from the environment. It is often assumed that the high-frequency active electrosense provides the key signals for prey-capture behavior. However, there is no direct evidence to support this assumption in South American gymnotids, and few studies address this question in African mormyrids (von der Emde, 1994; von der Emde and Bleckmann, 1998). It is possible that other nonvisual modalities, such as the low-frequency electrosense and the lateral line mechanosense, may contribute to prey-capture behavior. First, we outline candidate sensory modalities that may contribute to prey capture and provide evidence that electrosensory contributions are likely to dominate over the range of water conductivities encountered by the animal in its natural environment. Second, we discuss our findings concerning the positioning of peripheral electroreceptor surfaces, the functional importance of the dorsal surface and the evidence for a previously undescribed electrosensory orienting response. Finally, we discuss evidence that *Apteronotus* is able to modify its trajectory dynamically to capture moving prey. This finding implies that the nervous system implements a closed-loop control strategy during prey strikes.

Candidate sensory modalities supporting prey capture in Apteronotus

These studies were conducted under infrared illumination at a wavelength beyond the range of teleost photoreceptors (Douglas and Hawryshyn, 1990; Fernald, 1988), and our fish did not exhibit a startle response to the infrared illuminators, as they did to visible light. Thus, it is unlikely that visual cues were available to aid the fish in prey detection. Tactile contributions can be eliminated because detection always occurred when the prey was well separated from the fish (Figs 5, 6). In principle, acoustic cues may contribute, but the small prey used in this study are unlikely to generate pressure waves of sufficient strength to provide whole-body accelerations or stimulate the ear *via* the swim bladder and Weberian ossicles. Although chemosensory cues may stimulate feeding behavior, it is unlikely that the olfactory system can provide the spatial accuracy required to guide the precise high-efficiency strikes that were observed (Fig. 8).

The remaining candidate modalities that may contribute to prey detection are the high-frequency electrosense, the low-frequency electrosense and the lateral line mechanosense. These three sensory modalities are all part of the octavolateral system.

Dependence of detection distance on water conductivity

The key evidence that the electrosensory system is important for prey-capture behavior in *Apteronotus* comes from our observation of better detection performance (longer detection distances and lower miss rates) at lower water conductivities (Figs 7, 8). The mean detection distance nearly doubled (from 1.5 to 2.8 cm) between high-conductivity (600 μS cm^{-1}) and low-conductivity (35 μS cm^{-1}) conditions, and the miss rate decreased from 11 to 2 % in *A. albifrons*.

Natural conductivity ranges for Apteronotus

The conductivities of South American rivers and streams where *Apteronotus* is found (Ellis, 1913) vary from minima of approximately 10 μS cm^{-1} in electrolyte-poor blackwater regions to typical values of 60–110 μS cm^{-1} in whitewater regions of Central Amazon (Crampton, 1998; Furch, 1984b). *Apteronotus* is also found in the relatively electrolyte-rich waters of the Western Amazon, with conductivities of 160–270 μS cm^{-1} (Hagedorn and Keller, 1996). Although

seasonal variations in conductivity in areas inhabited by weakly electric fish have been discussed in the literature (Kirschbaum, 1979; Hopkins, 1972; Knudsen, 1974), there does not appear to be significant seasonal variation in water conductivity for the fast-flowing waters inhabited by *Apteronotus* (Crampton, 1998; Furch, 1984a; Hagedorn, 1988; M. Hagedorn, personal communication).

In this study, we observed the best detection performance at the lowest conductivity ($35\,\mu S\,cm^{-1}$), which is within the natural range. Reduced performance was observed at the higher conductivities (300 and $600\,\mu S\,cm^{-1}$) that are probably outside the natural range.

Effects of water conductivity on high-frequency electrolocation

Changes in water conductivity can influence high-frequency (active) electrolocation performance in three ways: effects on the fish's EOD strength, effects on tuberous receptor sensitivity, and effects on the 'electrical contrast' between an object and the surrounding water.

The first effect is due to the constant-current source characteristic of the electric organ of *A. albifrons*, which causes the EOD amplitude to increase with increasing water resistivity (Knudsen, 1975). On the basis of data presented by Knudsen (Knudsen, 1975), we estimate that the EOD amplitude was approximately 10 times higher at our lowest conductivity ($35\,\mu S\,cm^{-1}$) than at our highest water conductivity ($600\,\mu S\,cm^{-1}$). The strength of the voltage perturbation induced by the *Daphnia* is proportional to the strength of the fish's own electric field (Rasnow, 1996). Hence, considering only the effect of bath conductivity on EOD amplitude, we expect the intensity of the *Daphnia* image on the skin to increase as water conductivity is decreased. Other studies of weakly electric fish have also established that performance in certain high-frequency electrolocation tasks improves with lowered bath conductivity, including the ability to discriminate capacitative targets (von der Emde, 1993) and the distance at which conspecifics are detected (Moller, 1995; Squire and Moller, 1982).

The second effect of water conductivity on high-frequency electrolocation is related to changes in tuberous receptor organ sensitivity. Knudsen (Knudsen, 1974) found that behavioral thresholds to high-frequency stimuli increased with decreasing water conductivity in *Apteronotus*. On the basis of Knudsen's data (Fig. 7 in Knudsen, 1974), we would expect the behavioral threshold for an active electrolocation stimulus to increase by a factor of approximately three as water conductivity decreases from the highest conductivity used in our study to the lowest. This change in sensitivity is measured in terms of an externally imposed voltage gradient in the water outside the skin and it is independent of the change in amplitude of the fish's EOD discussed above.

The third effect is related to the electrical contrast of the prey. The magnitude of the active electrolocation stimulus depends on the degree to which the electrical impedance of an object differs from that of the surrounding medium (Rasnow, 1996). We have found that the resistive impedance of *Daphnia* approximately matches that of the surrounding water at a bath conductivity of $300\,\mu S\,cm^{-1}$ (M. A. MacIver and M. E. Nelson, unpublished data). Considering only the resistive impedance of the prey, we would expect its electrical contrast to increase for conductivities both above and below $300\,\mu S\,cm^{-1}$.

In summary, as conductivity decreases from 600 to $35\,\mu S\,cm^{-1}$, we would expect an order of magnitude increase in the strength of the perturbation due to the current source property of the electric organ, a factor of three decrease in the overall sensitivity of peripheral electroreceptors and an increase in the electrical contrast of the prey. The net result is that lower conductivities should result in better performance for the high-frequency electrosense, and thus longer detection distances, to the extent that active electrolocation contributes to prey-capture behavior.

Effects of water conductivity on low-frequency electrolocation

Aquatic prey such as *Daphnia* generate weak low-frequency bioelectric fields (Wilkens et al., 1997; Peters and Bretschneider, 1972; Kalmijn, 1974) that can be sensed by the ampullary electroreceptors of weakly electric fish (Dunning, 1973; Zakon, 1986). Although the density of ampullary receptors on the surface of the body of *A. albifrons* is more than an order of magnitude lower than that of tuberous receptors, low-frequency electrolocation may well be important in prey-capture behavior. For example, Kalmijn and Adelman (reported in Kalmijn, 1974) found that *A. albifrons* and *Gymnotus carapo* will strike at low-frequency signal sources designed to mimic the bioelectric field of natural prey.

Changes in water conductivity can influence low-frequency electrolocation in two ways: effects on the bioelectric potential of the prey, and effects on the behavioral threshold of the fish. The first effect is due to the current source characteristic of *Daphnia*, causing in increasing bioelectric field strength with increasing water resistivity. The bioelectric potential of *Daphnia* at 1 mm distance has been measured to be of the order of a few hundred microvolts in low-resistivity water ($760\,\mu S\,cm^{-1}$) and several thousand microvolts in high-resistivity water ($10\,\mu S\,cm^{-1}$) (Wilkens et al., 1997; Wojtenek et al., 2000; W. Wojtenek and L. A. Wilkens, personal communication). The second effect was studied by Knudsen (Knudsen, 1974), who examined behavioral thresholds of *A. albifrons* to externally imposed low-frequency (10 Hz) sinusoidal fields at different water conductivities. Threshold values were lowest (approximately $0.6\,\mu V\,cm^{-1}$ peak-to-peak) at $100\,\mu S\,cm^{-1}$, and they increased modestly both above and below this conductivity to values of the order of $1.0–1.5\,\mu V\,cm^{-1}$ peak-to-peak over the range of conductivities of interest here ($35–600\,\mu S\,cm^{-1}$).

Of these two conductivity effects on low-frequency electrolocation, the order of magnitude increase in *Daphnia* field strength is expected to dominate the factor 2–3 increase in behavioral threshold. The net result is that lower water conductivity should result in better performance for the low-frequency electrosense, just as it did for the high-frequency electrosense.

Effects of water conductivity on the mechanosensory lateral line

Several species of non-electric fish use the mechanosensory lateral line for detecting the weak flow fields produced by prey (Montgomery, 1989; Bleckmann et al., 1991; Enger et al., 1989; Montgomery and Milton, 1993; Janssen, 1997; Bleckmann, 1986; Kirk, 1985). Lateral-line-mediated detection distances for *Daphnia* are generally found to be approximately 1 cm (Coombs and Janssen, 1989; Janssen et al., 1995; Hoekstra and Janssen, 1986), although distances of up to 4 cm have been reported for a blind cave fish (*Typhlichthys subterraneus*), a mechanosensory specialist (Poulson, 1963).

Changes in water conductivity are not expected to influence mechanosensory sensitivity, except at very low conductivities, at which a low concentration of Ca^{2+} in the bath has been shown to reduce hair cell sensitivity (Crawford et al., 1991; Sand, 1975). We would expect to see such results only at our lowest conductivity ($35\,\mu S\,cm^{-1}$), at which the concentration of Ca^{2+} was $0.11\,mmol\,l^{-1}$. Studies with non-electric fish also suggest that lateral line sensitivity should be reduced at this Ca^{2+} concentration (Hassan et al., 1992; Sand, 1975). If mechanosensory cues were dominant in prey detection, we would expect detection performance to be largely insensitive to changes in water conductivity or, perhaps, to decrease with lower water conductivity because of the effects of low Ca^{2+} concentration.

To summarize, the improvement in detection performance that we observed at lower water conductivity strongly suggests that electrosensory cues dominate at the low conductivities. Best performance was observed at conductivities comparable with those experienced by the animal in its natural environment, leading us to conclude that the electrosense is the ecologically relevant sensory modality for prey capture.

Our results leave open the possibility that improved prey-capture performance for both species at low conductivities could be due to either high- or low-frequency components of the electrosense. To assess whether one component is more likely to dominate, we compared estimated signal strengths with estimated behavioral thresholds. Both the high- and low-frequency signal strengths appeared to be of the right order of magnitude to be detectable at the observed prey detection distances. Determining the relative contributions of these two components will therefore require further investigation.

Functional importance of the dorsal receptor surface

The dorsal surface of the fish appears to be of particular functional importance during prey-capture behavior. When searching for prey, the fish typically swam forward with an upright posture (i.e. with a roll angle near zero) and with its body pitched downwards such that the dorsum formed the leading edge as the fish moved through the tank. Furthermore, immediately following detection, the fish initiated a rolling movement during the reversal that brought the *Daphnia* more directly above the dorsum. Figs 5 and 6 show that the active space for prey detection is a wedge of space above the dorsum that extends along the entire length of the body. The observed dorsal bias may in part be due to the prey drifting downwards from the point of introduction near the water surface. Previous studies of active electrolocation in gymnotids have often focused on objects placed lateral to the fish's flattened body surface, but our results suggest that the space above the dorsum may have greater functional importance to the animal, at least under the conditions of our study.

The functional importance of the dorsum is also reflected by regional specializations in electroreceptor distribution on the body surface (Carr et al., 1982). The distribution of tuberous receptors is 2–3 times more dense on the dorsal surface of the trunk than on the lateral surface. A similar dorsal bias is observed for ampullary receptors. In contrast, the mechanosensory system has a more lateral bias, with the majority of the neuromasts on the trunk located in the lateral line; only a few superficial (non-canal) neuromasts are located on the dorsum. Apteronotids also possess a specialized electrosensory structure on the dorsal midline, known as the dorsal filament, that may aid in the detection and discrimination of prey (Franchina and Hopkins, 1996). In *A. albifrons*, this filament extends along the caudal-most third of the dorsum. Given that the EOD field is stronger near the tail (Rasnow and Bower, 1996) and given the presence of the dorsal filament, we might expect a bias in the detection point distribution towards this region. However, we did not observe this (Fig. 6B,C), perhaps in part because the tail region has a smaller surface area and fewer receptors, and perhaps because the fish was not required to discriminate prey from other objects in this study.

Roll: evidence for an electrosensory orienting response to prey

We observed that following detection the fish executed a body roll to position the prey more directly above the dorsum (Figs 9, 10A). This rolling behavior may have both sensory and biomechanical aspects. The sensory aspect is similar to an orienting response observed in Mexican blind cave fish in which the fish rolls the lateral side of its body, and thus the lateral line canal organs, towards objects (von Campenhausen et al., 1981). For *Apteronotus*, in addition to taking advantage of the dorsal electrosensory specializations discussed above, centering the prey above the dorsum may facilitate spatial localization by allowing comparisons between electroreceptor activation on the left and right sides of the body. A balanced stimulus would indicate that the prey was located directly above the dorsum, whereas an imbalance could serve as a relative measure of the angular deviation from the dorsal plane. In the weakly electric gymnotid *Eigenmannia virescens*, Feng (Feng, 1977) observed that the roll component of the substrate-orienting response was abolished by sectioning one of the bilateral trunk electroreceptor nerves, suggesting that the roll response may depend on bilateral electrosensory comparisons. Balancing an electrosensory stimulus on two sides of the body has also been reported in *Gymnotus carapo* for spatial localization of an electrical dipole (Hopkins et al., 1997). In general, localization through bilateral comparison of stimulus intensity is a common orienting strategy (Kuc, 1994; Hinde, 1970; Coombs and Conley, 1997).

The biomechanical aspect of dorsal roll is related to hydrodynamic constraints associated with the knife-like shape of the animal and the propulsive capabilities of the ribbon fin. Because of these constraints, the fish cannot perform pure lateral translations. Thus, when the initial prey position has a lateral component, the optimal approach strategy may be a dorsal roll towards the prey accompanied by a dorsum-leading reversal. Similar hydrodynamic constraints have been noted for movements of the flattened rostrum of the paddlefish during prey capture (Wilkens et al., 1997; L. A. Wilkens, personal communication). The electrosensory specialization of the dorsal body surface in *Apteronotus* may have evolved as a result of these biomechanical and hydrodynamic constraints on movement.

Backward swimming

Historically, backward swimming in electric fish has been a topic of keen interest and speculation, triggering research that led to Lissmann's discovery of active electrolocation (Lissman, 1958; Moller, 1995). Our results show that rapid reversals in swimming direction play a key role in the behavioral strategy used by *Apteronotus* for prey capture (Fig. 3), as has been reported previously for several gymnotids (Heiligenberg, 1973; Lannoo and Lannoo, 1993; Nanjappa et al., 2000).

For fish that detect prey using the electrosense, there are two general body designs and two corresponding behavioral strategies that permit efficient prey capture. The first design has the mouth located subterminally, with receptors in front, allowing prey to be scanned across the receptor array before reaching the mouth during forward swimming. This is observed in many elasmobranchs and in paddlefish (Wilkens et al., 1997; Montgomery, 1991). The second design has the mouth positioned terminally, with receptors located behind the mouth. This design is complemented with a behavioral strategy of backward swimming to scan the image across the receptor array, as observed in *Apteronotus* and other gymnotids (Heiligenberg, 1973; Lannoo and Lannoo, 1993; Nanjappa et al., 2000). In *Apteronotus*, tuberous and ampullary electroreceptor densities are approximately 5–10 times higher on the head than on the trunk (Carr et al., 1982); the head can therefore be considered to be the 'electrosensory fovea'. By executing a rapid reversal, the fish scans the electric image of the *Daphnia* across a receptor array of increasing density and provides the animal with a progressively stronger and sharper electrosensory perception.

Tail bending

Swimming modes that utilize propagated waves along an elongated ventral (gymnotiform mode) or dorsal (amiiform mode) ribbon fin effectively decouple locomotion from trunk movements (Breder, 1926). Lissmann (Lissmann, 1958; Lissmann, 1961), among others, has speculated that ribbon fin locomotion, when performed with a rigid trunk, may help electric fish avoid electrosensory reafference caused by tail bending (Bastian, 1995; von Holst and Mittelstaedt, 1950). Tail bends cause large modulations of the transdermal potential due to movement of the electric organ in the tail (Assad, 1997; Bastian, 1995). It is also possible that, by decoupling propulsion from trunk movement, trunk movement can be utilized to aid sensory acquisition. For example, gymnotids are known to execute nonlocomotory tail bends during exploration of novel objects (Heiligenberg, 1975; Assad et al., 1999). Lannoo and Lannoo (Lannoo and Lannoo, 1993) noted that *A. albifrons* arched its body towards *Daphnia* during prey-capture behavior. The gymnotid *G. carapo* also bends its body to conform to the curvature of electric field lines when approaching dipole sources (Hopkins et al., 1997).

We examined tail bending in *A. albifrons* during prey-capture behavior to address some of these issues. We observed that the fish does not keep its body straight prior to detection (Fig. 12), arguing against the need to minimize electrosensory reafference by maintaining a straight trunk. It is now known that fish can compensate for electrosensory reafference in the central nervous system (Bastian, 1995; Bastian, 1999). We did note that the RMS value of the bend angle dropped significantly following detection (Fig. 12), which implies a straightening of the body during the rapid reversal. This may have sensory relevance or may be due to hydrodynamic constraints on rapid backward movements.

In addition to examining the magnitude of tail bending, we quantified the velocity of tail bending. Our results show an average RMS bending velocity close to $107\,^{\circ}\,s^{-1}$, corresponding to an arc velocity of approximately $19\,cm\,s^{-1}$ at the tip of the tail. The tail-bending behavior we observed is different from the slow, large-amplitude 'tail probing' that occurs during exploration of novel objects (Assad et al., 1999). In general, the tail bends we observed were fast, small-amplitude adjustments of body posture. It is possible that these postural adjustments facilitate active electrolocation by modulating the spatiotemporal properties of the electric image of the *Daphnia*.

Closed-loop control of prey capture

Our results show that, following prey detection, *Apteronotus* is able to modify its trajectories adaptively to intercept prey that are drifting or being buffeted away. Closed-loop control of prey capture is rather remarkable given how rapidly the behavior is executed, with a mean time from detection to capture of $665\pm165\,ms$. Thus, it appears that the fish continues to process incoming electrosensory data and update estimates of current prey position on a relatively fast time scale. Another possibility is that the fish is able to predict the trajectory of the prey and use this prediction for feedforward control of the prey-capture strike. We believe this is unlikely in this case, because the majority of the movement of the prey appears to be due to turbulence caused by the fish's rapid reversal, the effects of which could be quite difficult to predict. The real-time demands of closed-loop tracking of prey set limits on the integration times that the nervous system uses for prey localization and therefore constrain neural models of electrosensory target acquisition. Such a closed-loop strategy is similar to the nonvisual prey pursuit strategies observed in echolocating bats (Kalko, 1995), and it contrasts with open-loop, ballistic strike strategies such as those observed in the tiger beetle (Gilbert, 1997) and mottled sculpin (Coombs and Conley, 1997).

We are grateful to Stuart Levy for his role in bringing the model-based tracking data into the virtual reality CAVE. We thank Brian Rasnow and Chris Assad for helpful discussions regarding the field of *Apteronotus*, and Lon Wilkens and Winfried Wojtenek for data on the bioelectric potentials of *Daphnia*. We also thank Ben Grosser and the staff of the Visualization, Media, and Imaging Laboratory at the Beckman Institute of Advanced Science Technology for assistance with video digitizing. This research was supported by a grant from the National Institute of Mental Health (R01MH49242).

References

Assad, C. (1997). Electric field maps and boundary element simulations of electrolocation in weakly electric fish. PhD thesis, California Institute of Technology.

Assad, C., Rasnow, B. and Stoddard, P. K. (1999). Electric organ discharges and electric images during electrolocation. *J. Exp. Biol.* **202**, 1185–1193.

Bastian, J. (1986). Electrolocation: behavior, anatomy and physiology. In *Electroreception* (ed. T. H. Bullock and W. Heiligenberg), pp. 577–612. New York: Wiley.

Bastian, J. (1995). Pyramidal-cell plasticity in weakly electric fish: a mechanism for attenuating responses to reafferent electrosensory inputs. *J. Comp. Physiol.* A **176**, 63–78.

Bastian, J. (1999). Plasticity of feedback inputs in the apteronotid electrosensory system. *J. Exp. Biol.* **202**, 1327–1337.

Bleckmann, H. (1986). Role of the lateral line in fish behaviour. In *Behaviour of Teleost Fishes*, second edition (ed. T. J. Pitcher), pp. 177–202. London: Chapman & Hall.

Bleckmann, H., Breithaupt, T., Blickhan, R. and Tautz, J. (1991). The time course and frequency content of hydrodynamic events caused by moving fish, frogs and crustaceans. *J. Comp. Physiol.* A **168**, 749–757.

Breder, C. M. (1926). The locomotion of fishes. *Zoologica* **4**, 159–297.

Carr, C. E., Maler, L. and Sas, E. (1982). Peripheral organization and central projections of the electrosensory nerves in gymnotiform fish. *J. Comp. Neurol.* **211**, 139–153.

Coombs, S. and Conley, R. A. (1997). Dipole source localization by mottled sculpin. I. Approach strategies. *J. Comp. Physiol.* A **180**, 387–399.

Coombs, S. and Janssen, J. (1989). Peripheral processing by the lateral line system of the mottled sculpin (*Cottus bairdi*). In *The Mechanosensory Lateral Line: Neurobiology and Evolution* (ed. S. Coombs, P. Gorner and H. Münz), pp. 299–319. New York: Springer-Verlag.

Crampton, W. G. R. (1998). Electric signal design and habitat preferences in a species rich assemblage of gymnotiform fishes from the Upper Amazon Basin. *Ann. Acad. Bras. Ci.* **70**, 805–847.

Crawford, A. C., Evans, M. G. and Fettiplace, R. (1991). The actions of calcium on the mechano-electrical transducer current of turtle hair cells. *J. Physiol., Lond.* **434**, 369–398.

Cruz-Neira, C., Sandin, D. J. and DeFanti, T. A. (1993). Surround-screen projection-based virtual reality: The design and implementation of the CAVE. *Computer Graphics (SIGGRAPH '93 Proceedings)* **27**, 135–142.

Cruz-Neira, C., Sandin, D. J., DeFanti, T. A., Kenyon, R. V. and Hart, J. C. (1992). The CAVE: Audio Visual Experience Automatic Virtual Environment. *Commun. ACM* **35**, 65–72.

Douglas, R. H. and Hawryshyn, C. W. (1990). Behavioral studies of fish vision: an analysis of visual capabilities. In *The Visual System of Fish* (ed. R. Douglas and M. Djamgoz), pp. 373–418. London: Chapman & Hall.

Dunning, B. B. (1973). A quantitative and comparative analysis of the tonic electroreceptors of *Gnathonemus*, *Gymnotus* and *Kryptopterus*. PhD thesis, University of Minnesota.

Ellis, M. M. (1913). The gymnotid eels of tropical America. *Mem. Carnegie Mus.* **6**, 109–195.

Enger, P. S., Kalmijn, A. J. and Sand, O. (1989). Behavioral investigation on the functions of the lateral line and inner ear in predation. In *The Mechanosensory Lateral Line: Neurobiology and Evolution* (ed. S. Coombs, P. Gorner and H. Münz), pp. 575–587. New York: Springer-Verlag.

Feng, A. S. (1977). The role of the electrosensory system in postural control of the weakly electric fish *Eigenmannia virescens*. *J. Neurobiol.* **8**, 429–438.

Fernald, R. D. (1988). Aquatic adaptations in fish eyes. In *Sensory Biology of Aquatic Animals* (ed. J. Atema, R. R. Fay, A. N. Popper and W. N. Tavolga), pp. 433–466. New York: Springer-Verlag.

Franchina, C. R. and Hopkins, C. D. (1996). The dorsal filament of the weakly electric Apteronotidae (Gymnotiformes: Teleostei) is specialized for electroreception. *Brain Behav. Evol.* **47**, 165–178.

Furch, K. (1984a). Seasonal variation of the major cation content of the várzea-lake Lago Camaleão, middle Amazon, Brazil, in 1981 and 1982. *Verh. Int. Verein. Limnol.* **22**, 1288–1293.

Furch, K. (1984b). Water chemistry of the Amazon basin: The distribution of chemical elements among freshwaters. In *The Amazon: Limnology and Landscape Ecology of a Mighty Tropical River and its Basin* (ed. H. Sioli), pp. 167–199. Dordrecht: Dr. W. Junk.

Gilbert, C. (1997). Visual control of cursorial prey pursuit by tiger beetles (Cicindelidae). *J. Comp. Physiol.* A **181**, 217–230.

Hagedorn, M. (1988). Ecology and behavior of a pulse-type electric fish *Hypopomus occidentalis* (Gymnotiformes, Hypopomidae) in a fresh-water stream in Panama. *Copeia* **1988**, 324–335.

Hagedorn, M. and Keller, C. (1996). Species diversity of gymnotiform fishes in Manu Bioreserve, Pakitza, Perú. In *Manu: the Biodiversity of Southeastern Perú* (ed. A. Sandoval and D. E. Wilson), pp. 483–502. Washington, DC: Smithsonian Institution.

Hassan, E.-S., Abdel-Latif, H. and Biebricher, R. (1992). Studies of the effects of Ca^{++} and Co^{++} on the swimming behavior of the blind Mexican cave fish. *J. Comp. Physiol.* A **171**, 413–419.

Heiligenberg, W. (1973). Electrolocation of objects in the electric fish *Eigenmannia* (Rhamphichthyidae, Gymnotoidei). *J. Comp. Physiol.* **87**, 137–164.

Heiligenberg, W. (1975). Theoretical and experimental approaches to spatial aspects of electrolocation. *J. Comp. Physiol.* **103**, 247–272.

Hinde, R. A. (1970). *Animal Behavior: A Synthesis of Ethology and Comparative Psychology*, pp. 146–192. New York: McGraw-Hill.

Hoekstra, D. and Janssen, J. (1986). Lateral line receptivity in the mottled sculpin (*Cottus bairdi*). *Copeia* **1**, 91–96.

Hopkins, C. D. (1972). Patterns of electrical communication among gymnotid fish. PhD thesis, Rockefeller University.

Hopkins, C. D., Shieh, K. T., McBride, D. W. and Winslow, M. (1997). A quantitative analysis of passive electrolocation behavior in electric fish. *Brain Behav. Evol.* **50** (Suppl. 1), 32–59.

Janssen, J. (1997). Comparison of response distance to prey *via* the lateral line in the ruffe and yellow perch. *J. Fish Biol.* **51**, 921–930.

Janssen, J., Jones, W. R., Whang, A. and Oshel, P. E. (1995). Use

of the lateral line in particulate feeding in the dark by juvenile alewife (*Alosa pseudoharengus*). *Can. J. Fish. Aquat. Sci.* **52**, 358–363.

Kalko, E. K. (1995). Insect pursuit, prey capture and echolocation in pipistrelle bats (Microchiroptera). *Anim. Behav.* **50**, 861–880.

Kalmijn, A. J. (1974). The detection of electric fields from inanimate and animate sources other than electric organs. In *Electroreceptors and Other Specialized Receptors in Lower Vertebrates. Handbook of Sensory Physiology*, vol. III/3 (ed. A. Fessard), pp. 147–200. Berlin: Springer.

Kirk, K. L. (1985). Water flows produced by *Daphnia* and *Diaptomus*: Implications for prey selection by mechanosensory predators. *Limnol Oceanogr.* **30**, 679–686.

Kirschbaum, F. (1979). Reproduction of the weakly electric fish *Eigenmannia virescens* (Rhamphichtyidae, Teleostei) in captivity. I. Control of gonadal recrudescence and regression by environmental factors. *Behav. Ecol. Sociobiol.* **4**, 331–355.

Knudsen, E. I. (1974). Behavioral thresholds to electric signals in high frequency electric fish. *J. Comp. Physiol.* **91**, 333–353.

Knudsen, E. I. (1975). Spatial aspects of the electric fields generated by weakly electric fish. *J. Comp. Physiol.* **99**, 103–118.

Kuc, R. (1994). Sensorimotor model of bat echolocation and prey capture. *J. Acoust. Soc. Am.* **96**, 1965–1978.

Lannoo, M. J. and Lannoo, S. J. (1993). Why do electric fishes swim backwards? An hypothesis based on gymnotiform foraging behavior interpreted through sensory constraints. *Env. Biol. Fish.* **36**, 157–165.

Leigh, J., Vasilakis, C. A., Defanti, T. A., Grossman, R., Assad, C., Rasnow, B., Protopappas, A., De Schutter, E. and Bower, J. M. (1995). Virtual reality in computational neuroscience. In *Virtual Reality Applications* (ed. H. Jones, J. A. Vince and R. A. Earnshaw), pp. 293–306. London: Academic Press.

Lissmann, H. W. (1958). On the function and evolution of electric organs in fish. *J. Exp. Biol.* **35**, 156–191.

Lissmann, H. W. (1961). Ecological studies on gymnotids. In *Bioelectrogenesis* (ed. C. Chagas and A. P. de Carvalho), pp. 215–223. Amsterdam: Elsevier.

MacIver, M. A., Lin, J. L. and Nelson, M. E. (1997). Estimation of signal characteristics during electrolocation from video analysis of prey capture behavior in weakly electric fish. In *Computational Neuroscience: Trends in Research 1997* (ed. J. Bower), pp. 729–734. New York: Plenum.

MacIver, M. A. and Nelson, M. E. (2000). Body modeling and model-based tracking for neuroethology. *J. Neurosci. Meth.* **95**, 133–143.

Marrero, C. (1987). Notas preliminares acerca de la historia natural de los peces del bajo llano. I. Comparación de los hábitos alimentarios de tres especies de peces Gymnotiformes, en el Río Apure (Edo Apure), Venezuela. *Rev. Hydrobiol. Trop.* **20**, 57–63.

Mérigoux, S. and Ponton, D. (1998). Body shape, diet and ontogenetic diet shifts in young fish of the Sinnamary River, French Guiana, South America. *J. Fish Biol.* **52**, 556–569.

Moller, P. (1995). *Electric Fishes: History and Behavior*. London: Chapman & Hall.

Montgomery, J. C. (1989). Lateral line detection of planktonic prey. In *The Mechanosensory Lateral Line: Neurobiology and Evolution* (ed. S. Coombs, P. Gorner and H. Münz), pp. 551–574. New York: Springer-Verlag.

Montgomery, J. C. (1991). 'Seeing' with nonvisual senses: mechanosensory and electrosensory systems of fish. *News Physiol. Sci.* **6**, 73–77.

Montgomery, J. C. and Milton, R. C. (1993). Use of the lateral line for feeding in the torrent fish (*Cheimarrichthys fosteri*). *N. Z. J. Zool.* **20**, 121–125.

Nanjappa, P., Brand, L. and Lannoo, M. J. (2000). Swimming patterns associated with foraging in phylogenetically and ecologically diverse American weakly electric teleosts (Gymnotiformes). *Env. Biol. Fish.* **58**, 97–104.

Naruse, M. and Kawasaki, M. (1998). Possible involvement of the ampullary electroreceptor system in detection of frequency-modulated electrocommunication signals in *Eigenmannia*. *J. Comp. Physiol.* A **183**, 543–552.

Nelson, M. E. and MacIver, M. A. (1999). Prey capture in the weakly electric fish *Apteronotus albifrons*: sensory acquisition strategies and electrosensory consequences. *J. Exp. Biol.* **202**, 1195–1203.

Peters, R. C. and Bretschneider, F. (1972). Electric phenomena in the habitat of the catfish *Ictalurus nebulosus* LeS. *J. Comp. Physiol.* **81**, 345–362.

Poulson, T. L. (1963). Cave adaptation in amblyopsid fishes. *Am. Midl. Nat.* **70**, 257–290.

Rasnow, B. (1996). The effects of simple objects on the electric field of *Apteronotus*. *J. Comp. Physiol.* A **178**, 397–411.

Rasnow, B. and Bower, J. M. (1996). The electric organ discharges of the gymnotiform fishes. I. *Apteronotus leptorhynchus*. *J. Comp. Physiol.* A **178**, 383–396.

Ratnam, R. and Nelson, M. E. (2000). Nonrenewal statistics of electrosensory afferent spike trains: implications for the detection of weak sensory signals. *J. Neurosci.* **20**, 6672–6683.

Sand, O. (1975). Effects of different ionic environments on the mechano-sensitivity of lateral line organs in the mudpuppy. *J. Comp. Physiol.* **102**, 27–42.

Squire, A. and Moller, P. (1982). Effects of water conductivity on electrocommunication in the weak-electric fish *Brienomyrus niger* (Mormyriformes). *Anim. Behav.* **30**, 375–382.

von Campenhausen, C., Riess, I. and Weissert, R. (1981). Detection of stationary objects by the blind cave fish *Anoptichthys jordani* (Characidae). *J. Comp. Physiol.* **143**, 369–374.

von der Emde, G. (1993). The sensing of electrical capacitances by weakly electric mormyrid fish: effects of water conductivity. *J. Exp. Biol.* **181**, 157–173.

von der Emde, G. (1994). Active electrolocation helps *Gnathonemus petersii* to find its prey. *Naturwissenschaften* **81**, 367–369.

von der Emde, G. (1999). Active electrolocation of objects in weakly electric fish. *J. Exp. Biol.* **202**, 1205–1215.

von der Emde, G. and Bleckmann, H. (1998). Finding food: senses involved in foraging for insect larvae in the electric fish *Gnathonemus petersii*. *J. Exp. Biol.* **201**, 969–980.

von Holst, E. and Mittelstaedt, H. (1950). Das Reafferenzprinzip. *Naturwissenschaften* **37**, 464–476.

Wilkens, L. A., Russell, D. F., Pei, X. and Gurgens, C. (1997). The paddlefish rostrum functions as an electrosensory antenna in plankton feeding. *Proc. R. Soc. Lond. B* **264**, 1723–1729.

Winemiller, K. O. and Adite, A. (1997). Convergent evolution of weakly electric fishes from floodplain habitats in Africa and South America. *Env. Biol. Fish.* **49**, 175–186.

Wojtenek, W., Hofmann, M. H. and Wilkens, L. A. (2000). Primary afferent sensory neurons represent paddlefish natural prey. *Neurocomputing* (in press).

Zakon, H. H. (1986). The electroreceptive periphery. In *Electroreception* (ed. T. H. Bullock and W. Heiligenberg), pp. 103–156. New York: Wiley.